Fumaric Acid Production in *Saccharomyces cerevisiae* by *In Silico* Aided Metabolic Engineering

Guoqiang Xu[1,2,3], Wei Zou[1,2,3], Xiulai Chen[1,2], Nan Xu[1,2], Liming Liu[1,2,3]*, Jian Chen[1,2,3]*

1 State Key Laboratory of Food Science and Technology, Jiangnan University, Wuxi, China, 2 The Key Laboratory of Industrial Biotechnology, Ministry of Education, School of Biotechnology, Jiangnan University, Wuxi, China, 3 The Key Laboratory of Carbohydrate Chemistry and Biotechnology, Ministry of Education, School of Biotechnology, Jiangnan University, Wuxi, China

Abstract

Fumaric acid (FA) is a promising biomass-derived building-block chemical. Bio-based FA production from renewable feedstock is a promising and sustainable alternative to petroleum-based chemical synthesis. Here we report on FA production by direct fermentation using metabolically engineered *Saccharomyces cerevisiae* with the aid of *in silico* analysis of a genome-scale metabolic model. First, *FUM1* was selected as the target gene on the basis of extensive literature mining. Flux balance analysis (FBA) revealed that *FUM1* deletion can lead to FA production and slightly lower growth of *S. cerevisiae*. The engineered *S. cerevisiae* strain obtained by deleting *FUM1* can produce FA up to a concentration of 610 ± 31 mg L^{-1} without any apparent change in growth in fed-batch culture. FT-IR and ^{1}H and ^{13}C NMR spectra confirmed that FA was synthesized by the engineered *S. cerevisiae* strain. FBA identified pyruvate carboxylase as one of the factors limiting higher FA production. When the *RoPYC* gene was introduced, *S. cerevisiae* produced 1134 ± 48 mg L^{-1} FA. Furthermore, the final engineered *S. cerevisiae* strain was able to produce 1675 ± 52 mg L^{-1} FA in batch culture when the *SFC1* gene encoding a succinate–fumarate transporter was introduced. These results demonstrate that the model shows great predictive capability for metabolic engineering. Moreover, FA production in *S. cerevisiae* can be efficiently developed with the aid of *in silico* metabolic engineering.

Competing Interests: The authors have declared that no competing interests exist.

* E-mail: mingll@jiangnan.edu.cn (LML); jchen@jiangnan.edu.cn (JC)

Introduction

Fumaric acid (FA) is widely used in food, pharmaceutical and chemical industries, and is attracting increasing attention because it can be converted into therapeutic drugs and is a starting material for polymerization and esterification. FA is mainly produced petrochemically from maleic anhydride at present. Increasing petroleum prices, concerns about climate change and advances in the field of metabolic engineering have fueled renewed interest in the production of organic acids by microbial fermentation [1]. Although high FA yields have been obtained from fungi such as Rhizopus oryzae [2] and Rhizopus arrhizus [3], the process might be limited at the industrial scale because these fungi are difficult to grow and their morphology can strongly affect production characteristics. The yeast Saccharomyces cerevisiae was regarded as a suitable microorganism for biotechnological production of carboxylic acids [4], and significant progress has been made in exploring metabolic engineering for the production of carboxylic acids such as lactic [5], malic [6,7], and succinic acids [8,9] by S. cerevisiae.

At least two metabolic strategies can be used for FA production by S. cerevisiae. In the first, FA can be produced via a reductive tricarboxylic acid (TCA) cycle, which provides a maximum theoretical yield of 2 moles of FA per mole of glucose. Moreover,

this process involves biological CO_2 fixation instead of release, which is of great interest because of increasing concerns about climate change. In our previous study, an exogenous fumarate biosynthetic pathway involving reductive reactions of the TCA cycle was successfully introduced in S. cerevisiae via a series of simple genetic modifications and pyruvate carboxylase was identified as one of the factors limiting fumarate production [10]. However, the energy balance for FA synthesis via a reductive TCA cycle is barely even and does not provide any ATP for maintenance and active transport processes, and the redox balance is uneven. In the second strategy, FA can be produced via an oxidative TCA cycle and the engineered strain is stable in the fermentation process. It was reported that cells of a fumarase-deficient mutant accumulated extracellular FA when fermenting glucose [11]. Similarly, a concentration of 3.62 g L^{-1} at a yield of 0.11 moles of succinic acid per mole of glucose was achieved for oxidative production of succinic acid in yeast by deletion of the SDH1, SDH2, IDH1 and IDP1 genes [8].

Recent advances in genomics and other -omics technologies combined with computational analysis have opened new avenues for strain improvement [12–15]. Metabolic engineering combined with systems biology has been successfully applied to the development of strains capable of enhanced production of chemicals and materials by redistributing and optimizing meta-

bolic fluxes [16]. Identification of genes for manipulation is an essential step in metabolic engineering for strain improvement for enhanced production of target bioproducts.

In the present study, the target gene for FA production in S. cerevisiae was identified via literature mining. Then iND750, a validated genome-scale metabolic model (GSMM) of S. cerevisiae [17], was used for in silico simulation of the metabolic response to deletion of the target gene by flux balance analysis (FBA) [18] and robustness analysis (Figure 1) [19]. Rational metabolic engineering [20] was then applied to develop a S. cerevisiae strain capable of efficient FA production. In addition, to further improve FA production, the model combined with literature surveys was used as a tool to indentify the controlling steps, and experimental validation was performed.

Results

Target Selection and in silico Simulation

To search for target genes for FA production in S. cerevisiae, extensive mining of the literature on FA and S. cerevisiae was carried out. The results of this literature survey revealed that fumarase defects or FUM1 deletion can lead to FA production. Thus, FUM1 was selected as the target gene to be manipulated.

FBA analysis revealed that FUM1 deletion can lead to FA production at a rate of 0.357 mmol g^{-1} DCW h^{-1} for the modified model, whereas FA was not produced in the original iND750 model. Robustness analysis of the rates of D-glucose uptake and growth for the original and modified models showed that FUM1 deletion leads to slightly lower growth of S. cerevisae (Figure 2); the growth rate predicted for the modified model (0.954 h^{-1}) was only ~1.95% lower than for iND750 (0.973 h^{-1}). Thus, the in silico simulation indicated that FUM1 deletion should not only result in FA accumulation, but should also have no obvious influence on S. cerevisiae growth.

Strain Construction, Aerobic Batch Fermentation and FA Characterization

The fum1-deleted mutant was obtained by double-crossover replacement. To confirm that the disruption cassette was correctly integrated in the genome and replaced the target FUM1 gene, PCR analysis was performed using two primer sets (A and BM, and CM and D; Figure S1). To disrupt or overexpress other genes in a yeast strain for subsequent study, the gene disruption cassette can be removed from the genome so that the marker can be used a second time. Loss of the HIS marker was verified by appropriate PCR analysis using the primer sets A and BM, and CM and D (Figure S1).

To investigate the effects of FUM1 deletion on FA production, time profiles for growth characteristics, glucose consumption, FA production and ethanol formation were compared for the parent strain and the mutant. The mutant showed a slightly lower growth rate and ethanol formation compared to the parent strain. Moreover, the mutant accumulated FA to a concentration of up to 610±31 mg L^{-1} (yield of 0.018 moles of FA per mole of glucose) after 120 h of cultivation, while no FA was detected in the broth of parent strain during fermentation (Figure 3). The results are similar to those predicted by the S. cerevisiae iND750 GSMM.

The chemical structure of fumarate samples was confirmed by FT-IR and ^1H and ^{13}C NMR spectroscopy. IR spectra of samples and a fumarate standard were the same. Stretching vibrations of the carbonyl group were observed as strong bands at 1600 and 1850 cm^{-1}, while stretching vibrations of the hydroxyl group were observed as broad bands at 3200 and 2500 cm^{-1}(Figure S2). ^1H NMR spectra of a sample and the reference standard are shown in

Figure S3. The peak at 6.84 ppm was assigned to the CH proton, while the OH proton was substituted by deuterium from D_2O. ^{13}C NMR spectra of a fumarate sample and the reference standard are also shown in Figure S3. Both spectra show two signals, including two carboxylic carbons at 136.87 ppm, and two double-bonded carbons at 171.66 ppm. The results confirm that FA was synthesized by the engineered S. cerevisiae strain.

Strategies for Improving FA Production

To further improve FA production, key factors (such as enzymes) preventing channeling of the carbon flux to FA must be identified. First, the central metabolic flux of CEN.PK2-1CΔFUM1 was analyzed with cell growth as the objective when FA production successively increased from the control value (0.4 mmol g DCW h^{-1}) to the theoretical maximum value using iND750 and an FBA algorithm. According to the results, three types of intracellular flux profiles occur: increased, decreased and irregular (Table S1). As shown in Table 1, among the increased intracellular flux profiles, the carbon flux of pyruvate carboxylase increased more apparently with FA production, indicating that pyruvate carboxylase could be one of factors limiting higher FA production.

Effect of RoPYC Overexpression on FA Production

As an anaplerotic enzyme, cytosolic pyruvate carboxylase catalyzes the conversion of pyruvate to oxaloacetate. Kenealy et al. found high pyruvate carboxylase activity in a Rhizopus oryzae strain under aerobic conditions [3]. Thus, we investigated the effect of RoPYC overexpression, which encodes pyruvate carboxylase of R. oryzae, on FA production.

To test the hypothesis provided by the model, RoPYC overexpression in S. cerevisiae was investigated. The gene expression level of RoPYC was increased by 10-fold, as detected by quantitative real-time PCR (QT-PCR) (Figure 4). As shown in Figure 5, introduction of the RoPYC gene had a minimal effect on growth. However, the mutant FMME-002ΔFUM1+↑ RoPYC accumulated FA up to a concentration of 1134±48 mg L^{-1} within 96 h, representing an increase in FA of 86% compared with the parent strain. The rate of glucose consumption improved and the FA yield also increased when the RoPYC gene was introduced.

Improved FA Yield by Coexpression of RoPYC and SFC1

Efficient export of FA is also important to further enhance its production; on the contrary, insufficient transport capacity might impede efficient FA production. It has been reported that SFC1 encodes a succinate–fumarate transporter in S. cerevisiae [21–23].

Therefore, we investigated the potential of constitutive coexpression of RoPYC and SFC1 to further improve FA production. The gene expression levels of RoPYC and SFC1 were increased by 6-fold and 13-fold respectively (Figure 4). Results showed that additional introduction of SFC1 in the RoPYC overexpression strain lead to a slight increase in growth and glucose consumption and a significant improvement in FA production. The maximum FA concentration obtained was 1675±52 mg L^{-1} at 96 h, representing a 47.6% increase in comparison with the engineered strain FMME-002ΔFUM1+↑ RoPYC. However, as shown in Figure 6, no apparent difference was observed in glucose consumption rate between these two strains.

Thus, metabolic engineering of S. cerevisiae based on GSMM analysis and transporter engineering successfully yielded a genetically defined FA overproducer.
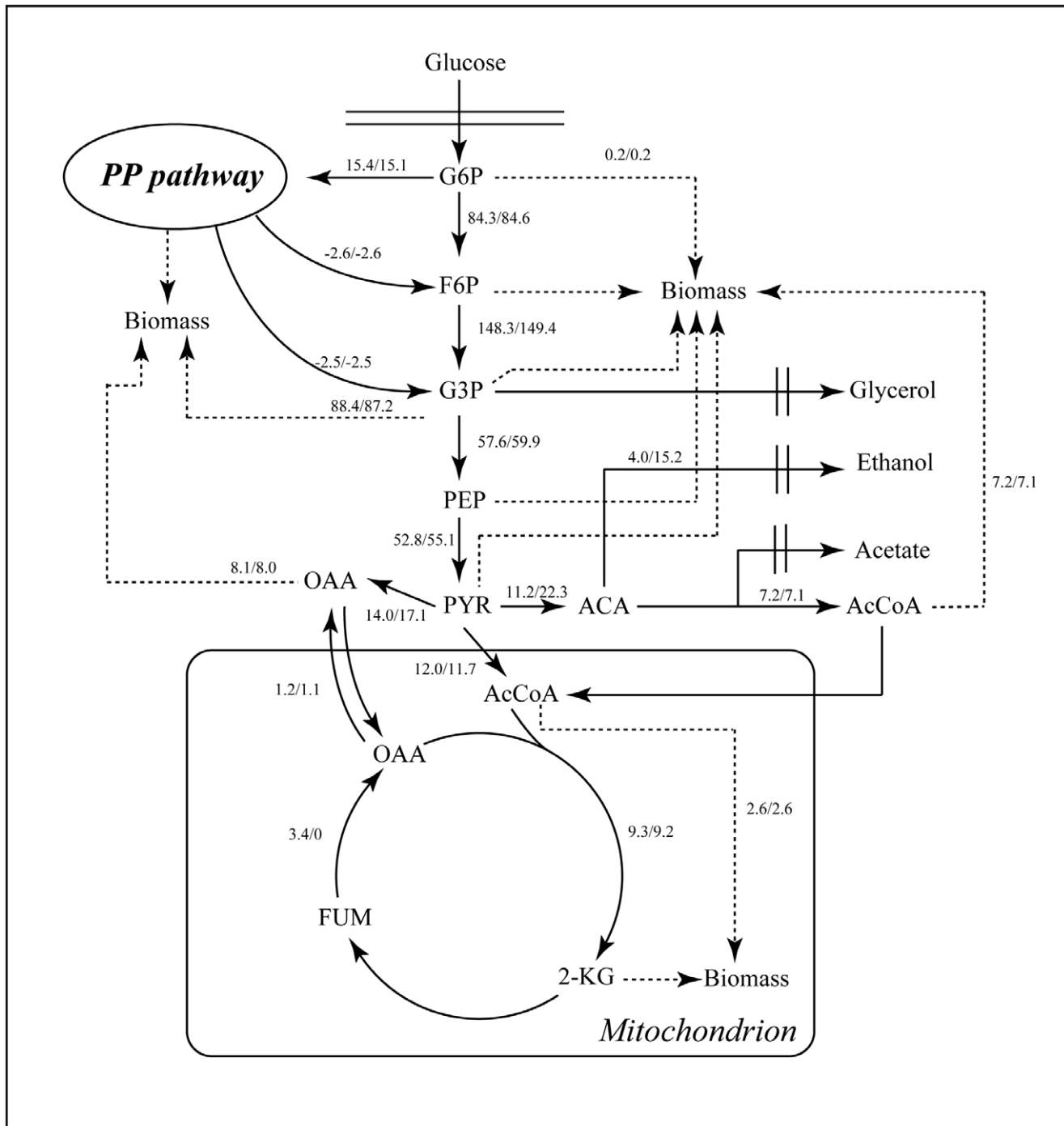
Figure 1. The major metabolic pathway leading to the formation of fumaric acid and *in silico* carbon flux distribution in the central metabolism of *S. cerevisiae* during fumaric acid production on glucose. a/b, "a" represent the flux of parent strain, "b" represent the flux of the mutant strain FMME-002ΔFUM1. Fluxes are shown relative to a glucose uptake rate of 100.
doi:10.1371/journal.pone.0052086.g001

Discussion

None of the natural fumarate-producing microorganisms seem to be suitable for large-scale commercial production although high FA yields have been obtained [2,3]. *S. cerevisiae* is an excellent platform for biologically based chemicals such as organic acids. The aim of the present study was to construct a genetically engineered *S. cerevisiae* strain that can produce FA. First, the target

gene *FUM1* was identified in an extensive literature search and then FBA was used to predict the effect of *FUM1* disruption using the *S. cerevisiae* iND750 GSMM. The simulated results revealed that *FUM1* deletion could lead to FA accumulation with only a slight influence on cell growth (~1.95% lower). Then gene deletion was carried out and engineered *S. cerevisiae* cells produced FA at concentrations up to 610 ± 31 mg L^{-1}. Meanwhile, cell growth and glucose consumption were slightly lower compared to
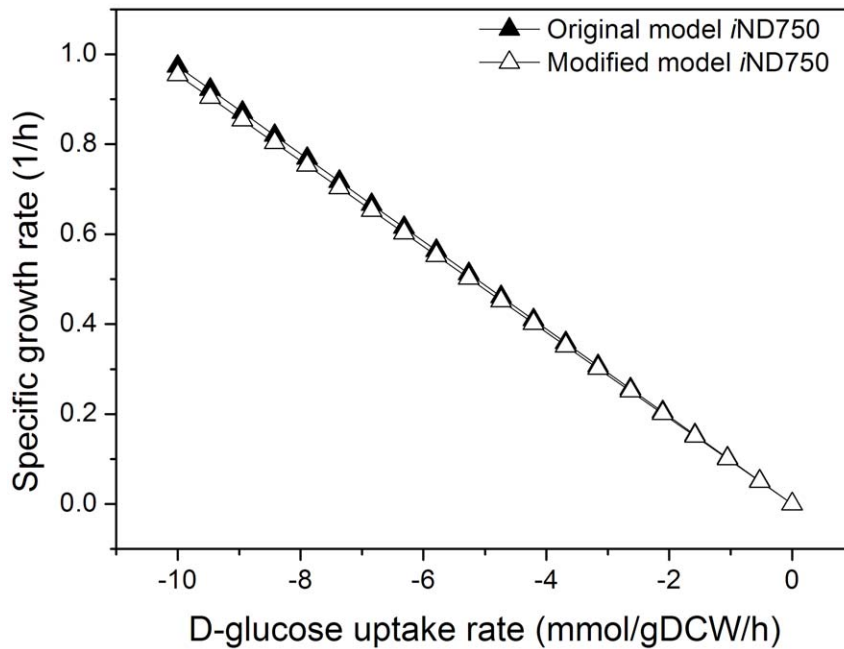
Figure 2. Robustness analysis for the D-glucose uptake rate and growth rate. Closed triangle represents the original model *i*ND750, open triangle represents the modified model *i*ND750.
doi:10.1371/journal.pone.0052086.g002

the parent strain, in accordance with the simulated result. Simulated results also showed that pyruvate carboxylase could be one of the factors limiting higher FA production, and an improved FA yield was obtained when the *RoPYC* gene was introduced. Furthermore, a significant improvement in FA production was achieved when the *SFC1* gene was introduced. The final FA concentration obtained was 1675 ± 52 mg L^{-1}. Thus, the engineered strain provides a potential new route for FA production. However, the concentration and yield are low in comparison with *R. oryzae* [2], so further work is required before this approach is economically feasible.

The number of GSMMs available is increasing sharply [24]. Because a GSMM represents nearly all the metabolic activities of an organism, it can be of great help in understanding metabolism on a global level [25]. Thus, GSMMs are widely used in metabolic engineering [26,27] and can be used to predict and evaluate genetic manipulations in advance (dry experiments) when combined with certain algorithms [18,28]. This can greatly improve the efficiency and directionality of metabolic engineering in various phases by predicting gene targets to be manipulated throughout the whole cellular network. In *S. cerevisiae*, metabolic engineering strategies aided by GSMM have led to improved production of various metabolites such as bioethanol, purine, proline/pyrimidines and vanillin [29]. In addition to direct improvements in production capacity, GSMMs can also be used to predict cellular properties or phenotypic traits such as growth and glucose consumption. In previous studies, growth behavior, and ethanol, succinate, citrate and fumarate concentrations were determined in various media (rich and minimal media) under aerobic and anaerobic conditions [11,30], but the effect of *FUM1* deletion or fumarase deficiency on fermentation profiles (growth and glucose uptake rate) has not been studied in detail. In the present study, the phenotypic trait of slightly lower growth caused by *FUM1* deletion in *S. cerevisiae* was successfully predicted by FBA analysis; this trait is important for metabolic engineering because unwanted side effects can be induced. Metabolic models are also

useful in identifying targets for further strain improvement. We identified pyruvate carboxylase as a factor restricting higher FA yield. A higher FA yield was obtained by increasing the flux through pyruvate carboxylase. The increased flux induced by overexpression of pyruvate carboxylase is linked to increased transport of cytosolic oxaloacetate into mitochondria and supply to oxidative reactions [31]. When pyruvate carboxylase and the transporter encoded by *SFC1* were coexpressed, a higher growth rate and FA yield were obtained, which suggests that insufficient FA export is another controlling step that would lead to higher FA production in steady-state metabolism.

The model showed some restrictions; however, the physiological characteristics observed for engineered organisms can be used to update the model. In the present study, there was very good accordance between *in silico* predictions and experimental results. The discrepancy between experimental and predictive yields was primarily caused by lack of model knowledge for yeast metabolism, regulatory mechanisms and feedback inhibition, which requires specific further experimental investigation.

In conclusion, the metabolic pathways in *S. cerevisiae* were rationally engineered for FA production with the aid of *in silico* simulations. The strategy described here can be useful for improved production of organic acids and other metabolites by direct microbial fermentation from renewable resources.

Materials and Methods

Strains and Plasmids

The strains and plasmids used are listed in Table 2. All yeast strains used were derived from strain *S. cerevisiae* CEN.PK2-1C (MATa ura3-52 leu2-3,112 trp1-289 his3Δ MAL2-8c SUC2), which was obtained from Euroscarf (Frankfurt, Germany). Plasmid pUG27 was constructed by replacing the *kanMX* marker in pUG6 with the his5$^+$ marker from pFA6a-HIS3MX6 (which complements the *S. cerevisiae his3* mutation) using *Bgl*II and *Sac*I restriction sites, as previously described [32]. *Pyrobest* DNA
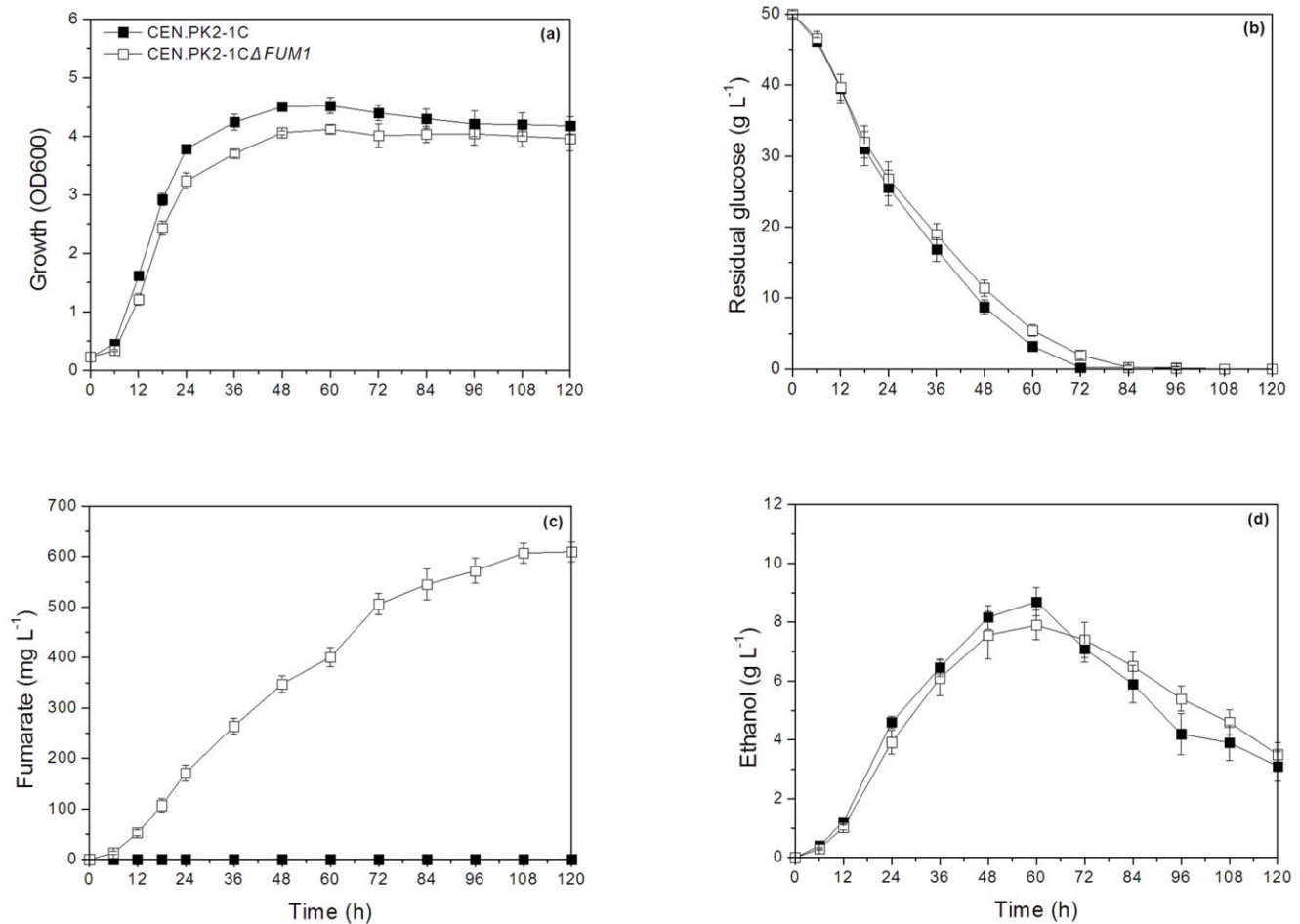
Figure 3. Fermentation profile for cell growth and product accumulation during aerobic batch culture. Closed square represents the parent strain, open square represents the mutant strain FMME-002ΔFUM1. (a): growth, (b): residual glucose, (c): fumaric acid, and (d): ethanol. Values are presented as means of three independent experiments. Bars represent the standard deviation.
doi:10.1371/journal.pone.0052086.g003

polymerase for PCR was purchased from TaKaRa Biotechnology (Dalian, China).

The Cre-expressing plasmid pSH47 was used for marker rescue [33]; the vector carries the cre-recombinase gene to remove the kanMX gene flanked by loxP sites, then the Cre plasmid pSH47 is removed from this yeast strain. Primers used in confirming the loss of selectable marker are listed in Table 3.

Literature Mining Method

To identify genes associated with FA production in *S. cerevisiae*, a literature search was carried out. The literature database consisted of articles downloaded from public online databases, including ScienceDirect (http://www.sciencedirect.com/), Springer Link(http://www.springerlink.com/), PubMed(http://www.ncbi. nlm.nih.gov/pubmed/), and ISI Web of Science (http://www.

Table 1. Flux analysis to select the gene amplification targets for enhanced fumaric acid production.

	Enzyme	Functional category	Folds
ENO	enolase	Glycolysis/Gluconeogenesis	1.44
GAPD	glyceraldehyde-3-phosphate dehydrogenase	Glycolysis/Gluconeogenesis	1.04
PGK	phosphoglycerate kinase	Glycolysis/Gluconeogenesis	1.04
PGM	phosphoglycerate mutase	Glycolysis/Gluconeogenesis	1.44
PYK	pyruvate kinase	Glycolysis/Gluconeogenesis	1.49
TPI	triose-phosphate isomerase	Glycolysis/Gluconeogenesis	1.04
PC	Pyruvate carboxylase	Anaplerotic reactions	1.82
ACONTm	Aconitate hydratase	Citric Acid Cycle	0.99

doi:10.1371/journal.pone.0052086.t001
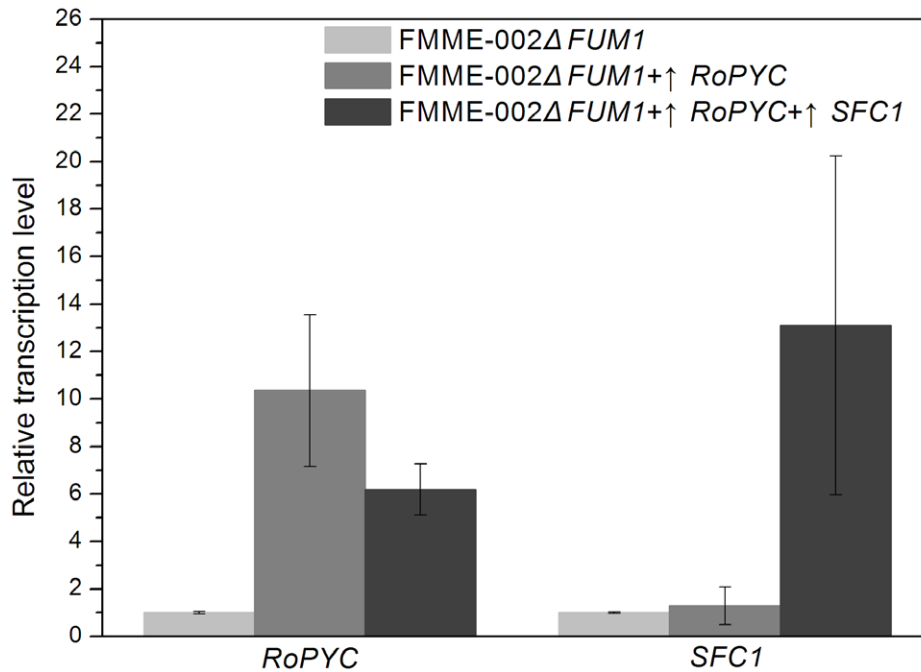
Figure 4. Relative gene expression levels. *RoPYC* and *SFC1* in the mutant strain FMME-002Δ*FUM1*, FMME-002Δ*FUM1*+↑ *RoPYC* and FMME-002Δ*FUM1*+↑ *RoPYC*+↑ *SFC1*, Relative transcription levels were normalized to the transcription level of the β-*ACTIN* gene, which was taken as 1. The presented values are averages of three independent experiments; the error bars indicate standard deviations.
doi:10.1371/journal.pone.0052086.g004

isiknowledge.com). Manual surveys of these papers were then carried out to obtain objective information.

Simulation of Single Gene Deletion

The impact of gene deletion on cell growth and FA production was evaluated *in silico* by FBA using the *S. cerevisiae* iND750 GSMM. To simulate single gene deletion, the flux of the reactions in iND750 catalyzed by target genes was set to zero (i.e., no flux). Then FBA was carried out to predict optimum growth in minimum medium in which D-glucose was the sole carbon source. The rate of D-glucose uptake was set to 10 mmol g^{-1} DCW h^{-1} and the biomass equation was taken as the objective function. The rates of growth and FA production were simulated and compared with values for the non-modified iND750 model under the same culture conditions. A robustness analysis of the rates of D-glucose uptake and growth between the original and modified models was also conducted. FBA simulations were performed using COBRA Toolbox v2.0 in MATLAB 2010b, with GLPK as the linear programming solver [34].

Construction of *S. cerevisiae* Deletion Strains

Deletion of the *FUM1* gene (1467 bp) was performed via a one-step inactivation method [33]. The vector pUG27 was used to delete this gene in *S. cerevisiae* CEN.PK2-1C. After plasmid preparation, a fragment of pUG27 was amplified by PCR to obtain a cassette consisting of *loxP*-*his5$^+$*-*loxP*. Primers were constructed (Table 3) to fuse 5′ and 3′ coding sequences of *FUM1* and sequences of the *loxP* regions of the pUG27 vector. The resulting PCR product comprised the *his5$^+$* gene, *loxP* sites and *FUM1* homologous regions for integrative transformation in *S. cerevisiae* CEN.PK2-1C. Homologous recombination in yeast led to deletion of the target gene. SC selection medium was prepared by adding a mixture of amino acids, purines and pyrimidines to Difco yeast nitrogen base, and histidine was omitted to select for positive

clones. Then the His marker was removed via transformation with pSH47. The vector carried the cre-recombinase gene to remove the *his5$^+$* gene flanked by *loxp* sites induced by 2% D-galactose. The Cre plasmid was subsequently removed from the yeast strain.

Plasmid Construction and Transformation

cDNA of *R. oryzae* NRRL1526 (ATCC 10260) was obtained as previously described [10]. Then PCR primer pairs covering the entire open reading frame of the *RoPYC* gene were designed according to GenBank sequences for *R. oryzae* using Primer Premier v5.0 software (Table 3). Thermal cycling was carried out as follows: the initial denaturation step was at 94°C for 5 min, followed by 29 cycles of denaturation at 94°C for 30 s, annealing at 52°C for 30 s, and extension at 72°C for 3.6 min, with a final single extension step at 72°C for 10 min. Then a 3540-bp fragment of the *RoPYC* gene was amplified by nested PCR. The sequence of this gene fragment was submitted to GenBank under accession number HM130700.1. Gene-specific primers were designed to amplify *RoPYC*, and *RoPYC* was then amplified by PCR using cDNA of *R. oryzae* NRRL1526 as a template. The resultant PCR fragment of *RoPYC* and expression vector pY15TEF1 were digested with SpeI and SalI and ligated together to create the pY15TEF1-*RoPYC* plasmid. The *S. cerevisiae* *SFC1* gene was amplified by PCR from chromosomal DNA of CEN.PK2-1C using the primers BamHI-F(*SFC1*) and HindIII-R(*SFC1*). The PCR fragment and pY26TEF-GPD vector were digested with BamHI and HindIII and ligated to create pY26TEF-GPD-*SFC1*.

Plasmids were introduced into yeast cells using a Frozen-EZ yeast transformation II kit (Zymo Research, Orange, CA, USA) according to manufacturer's protocol. Transformants were selected on agar plates of synthetic complete (SC) selection medium lacking leucine and uracil as auxotrophic markers.
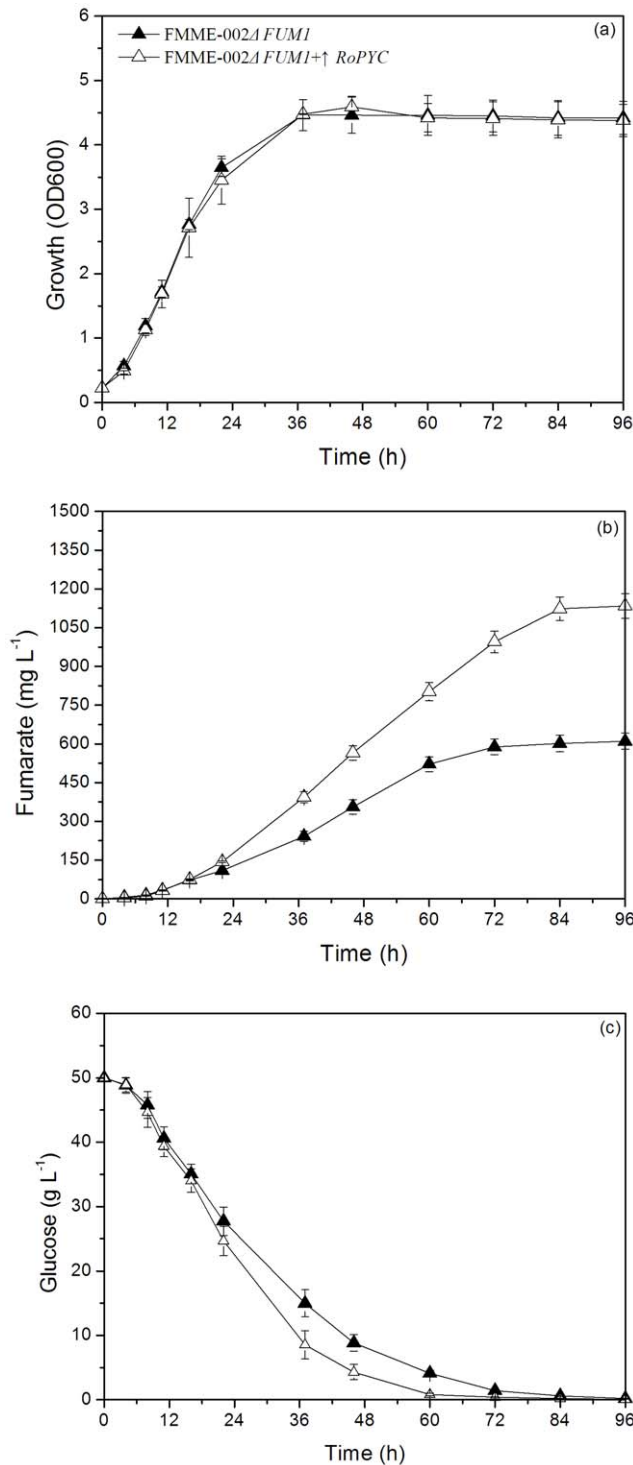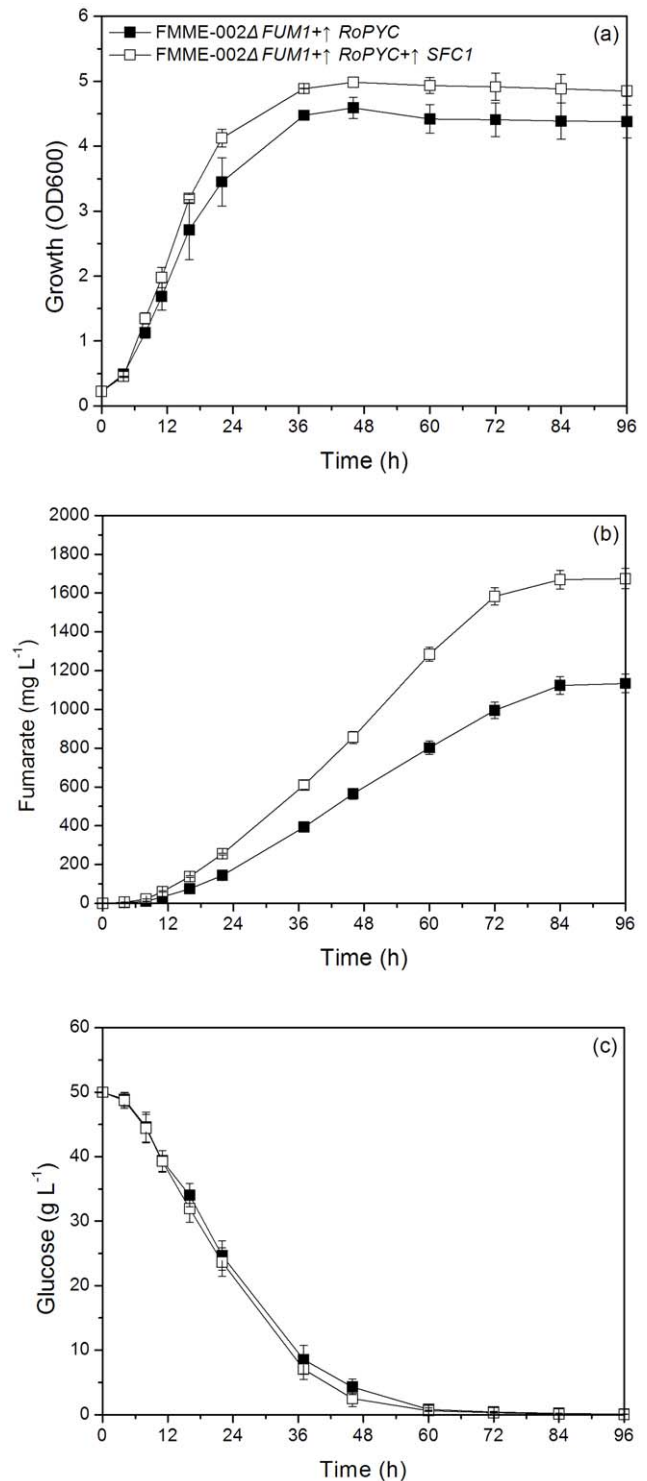
Figure 5. The effect of *RoPYC* over-expression on fermentation profile of engineered strain. Closed triangle represents the control strain FMME-002ΔFUM1, open triangle represents the mutant strain FMME-002ΔFUM1+ ↑ RoPYC. (a): growth, (b): fumaric acid, (c) : glucose. doi:10.1371/journal.pone.0052086.g005

Figure 6. The effect of *SFC1* and *RoPYC* co-expression on fermentation profile of engineered strain. Closed square represents the control strain FMME-002ΔFUM1+ ↑ RoPYC+ pY26TEF-GPD, open square represents the mutant strain FMME-002ΔFUM1+ ↑ RoPYC+ ↑ SFC1. (a): growth, (b): fumaric acid, (c): glucose. doi:10.1371/journal.pone.0052086.g006

Transcriptional Analysis

For RNA extraction, flask culture cells in early stationary phase were harvested by centrifugation (8000 rpm at 4°C for 5 min). Total RNA was isolated using an RNAprep pure plant kit according to the manufacturer's instructions. The amount of isolated RNA was determined photometrically (optical density at 260 nm [OD_{260}] of 1 equals 40 μg mL^{-1} RNA). Reverse transcription was carried out using an iScript^{TM} cDNA Synthesis Kit (Bio-Rad) according to the manufacturer's instructions.

Table 2. Strains and plasmids used in this study.

Strains and plasmids	Relevant characteristics	Source
Strains		
FMME-002	MATa; reference strain	Euroscarf
FMME-002ΔFUM1	MATa fum1::lox	This study
FMME-002ΔFUM1+ ↑ RoPYC	MATa fum1::lox{ pY15TEF1-RoPYC }	This study
FMME-002ΔFUM1+ ↑ RoPYC+ ↑ SFC1	MATa fum1::lox{pY15TEF1-RoPYC,pY26TEF-GPD-SFC1}	This study
Plasmids		
pFA6a-HIS3MX6	Amp,K.lactis HIS3	Lab collection
pUG27	Amp,K.lactis HIS3,loxp	This study
pSH47	Amp,GAL1-cre, URA3	Prof. Hegemann JH
pY15TEF1	Amp,LEU2	Lab collection
pY26TEF-GPD	2 μm URA3, P_{GPD}/T_{CYC1}, P_{TEF}/T_{ADH1}	Lab collection
pY15TEF1-RoPYC	Amp,LEU2,P_{TEF1}- RoPYC	This study
pY26TEF-GPD-SFC1	2 μm URA3, P_{GPD}/T_{CYC1}, P_{TEF}/T_{ADH1}, P_{GPD}-SFC1	This study

doi:10.1371/journal.pone.0052086.t002

Amplification of cDNA via quantitative real-time PCR was carried out using an iTaq^{TM} Universal SYBR Green Supermix Kit (Bio-Rad). The reaction mix consisted of 10 μL iTaq^{TM} Universal SYBR Green Supermix (2×), 1 μL each of forward and reverse primers (10 μmol), 2 μL of cDNA (50 ng), and 6 μL H_2O. Primers used in the transcriptional analysis are listed in Table 4. Amplication and detection of specific products were performed on a BIO-RAD® CFX96 system (Bio-Rad) according to following program: 95°C for 30 s, and 39 cycles of 95°C for 5 s, 55°C for 12 s. Data analysis was performed using the second derivative method, and expression levels were normalized to expression of the ACT1 reference gene. Each sample was tested in triplicate in a 96-well plate (Bio-Rad, Hercules, CA, USA).

Medium and Batch Fermentations

Luria-Bertani (LB) medium (5 g L^{-1} yeast extract, 10 g L^{-1} tryptone and 10 g L^{-1} NaCl) was used for plasmid purification from E. coli JM109. The fermentation medium (pH 5.0) contained (per liter) 50 g of glucose, 2 g of $CO(NH_2)_2$, 5 g of KH_2PO_4, 0.8 g of $MgSO_4·7H_2O$, and 10 mL of trace metal solution (0.2 g L^{-1} $MnCl_2·4H_2O$, 2 g L^{-1} $FeSO_4·7H_2O$, 2 g L^{-1} $CaCl_2·2H_2O$, 0.05 g L^{-1} $CuSO_4·5H_2O$, 0.5 g L^{-1} $ZnCl_2$). In flasks, 40 g L^{-1} $CaCO_3$ (dry-heat sterilized at 160°C for 30 min) was used as a buffer for the medium. Flasks were incubated at 30°C in an orbital shaker at 200 rpm. YPD medium (10 g L^{-1} yeast extract, 20 g L^{-1} peptone, 20 g L^{-1} glucose) was used for seed culture. The seed culture was inoculated with yeast growing well on an agar slant and was incubated for 24 h in a 250-mL flask containing 20 mL of

Table 3. Primers used in this study.

Primers	Sequence (5′-3′)	Usage
45-F(FUM1)	GAAATTCCATAAAGTCTAACTATTAAACGGATAAGAGATACAATC-CAGCTGAAGCTTCGTACGC	Disruption of FUM1
45-R(FUM1)	TTATTTAGGACCTAGCATGTGTTCAGGAACAACCCATTCATCAAA-GCATAGGCCACTAGTGGATCTG	
A(FUM1)	AATCTTCATCACTGTTGTAGACGTT	Confirming the loss of the HIS marker
B(FUM1)	GTTTTCAAAGAATGTGCCACTC	
C(FUM1)	TGCAAGTCATGGGTAACAATGC	
D(FUM1)	CTTAATAGGACTCAAATCGTGATGG	
B-M	GCCTGCTTGAATGCAATACC	
C-M	CACGAAGGGAGTGTTGTAAAGAG	
F(RoPYC)	ATGCCTGCTGCACCAGTAC	Cloning of RoPYC
R(RoPYC)	TTAGGCTTCCTCTTTGACAACC	
Spel-F(RoPYC)	GGACTAGT-ATGCCTGCTGCACCAGTAC	Construction of pY15TEF1-RoPYC
Sall-R(RoPYC)	ACGCGTCGAC-TTAGGCTTCCTCTTTGACAACC	
F(SFC1)	ATGTCTCAAAAAAAGAAGGCTTC	Cloning of SFC1
R(SFC1)	CTACTTTAATGGCTTTGGCTTTG	
BamHI-F(SFC1)	CGGGGATCC-ATGTCTCAAAAAAAGAAGGCTTC	Construction of pY26TEF-GPD-SFC1
HindIII-R(SFC1)	CCCAAGCTT-CTACTTTAATGGCTTTGGCTTTG	

doi:10.1371/journal.pone.0052086.t003

Table 4. Primers used in the transcriptional analysis.

Primer	Sequence, 5′-3′	Analyzed gene
F(RoPYC)	TGTTGAAGCCACCATCTG	RoPYC
R(RoPYC)	GCACGGATACTGAAGACC	
F(SFC1)	GGCAAGGCAAGCAACTAATCAG	SFC1
R(SFC1)	CCAATAGCACCCGAAATCAAACC	
F(ACT)	TTATTGATAACGGTTCTGGTATG	β-ACTIN
R(ACT)	CCTTGGTGTCTTGGTCTAC	

doi:10.1371/journal.pone.0052086.t004

seed medium. The broth was centrifuged, the pellet was resuspended in isometric fresh fermentation medium, and the cell suspension was inoculated into a 250-mL shaker flask containing 50 mL of fermentation medium.

Analytical Methods

Cell growth was monitored by measuring the absorbance at 600 nm (OD_{600}) spectrophotometrically. Cell concentration, defined as grams of dry cell weight (g DCW) per liter, was calculated from a standard curve relating OD_{600} to dry weight (1 OD_{600} = 0.35 g DCW L^{-1}). Extracellular concentrations of fumaric acid, ethanol and glucose were determined by HPLC using an Aminex HPX-87H column (Bio-Rad) eluted with 0.0275% (v/v) H_2SO_4 at a flow rate of 0.6 mL min^{-1} at 35°C. Fumaric acid was monitored using an Agilent (Santa Clara, CA, USA) 1200 series DAD detector at 210 nm. Ethanol and glucose were monitored using a 1200 series Agilent refractive index detector.

Confirmation of FA Biosynthesis by FT-IR and NMR

Cell cultures of the engineered strain were centrifuged and the supernatant was adjusted to pH 1.0 by addition of HCl. Following acidification, fumaric acid precipitated out of the solution and was recovered by drying in a rotary dryer. The sample obtained was processed in parallel with a fumaric acid reference standard for FT-IR and ^{1}H and ^{13}C NMR analyses. FT-IR spectra were recorded on a Nicolet Nexus 470 spectrophotometer with a DTGS detector. Fumarate samples and the reference standard were diluted in KBr and measured in transmittance mode over the spectral range 400–4000 cm^{-1}. ^{1}H NMR (400 MHz, D_2O, 25°C)

and ^{13}C NMR (100 MHz, D_2O, 25°C) spectra were recorded on an Avance III 400-MHz digital NMR spectrometer.

Supporting Information

Figure S1   PCR analysis to confirm correct integration of the HIS marker gene disruption cassette at the YPL262W locus and confirm the loss of selectable marker. The size of the expected PCR products is given below each lane. Wild type, nontransformed wild type yeast strain; Mutant I, mutant yeast strain carrying the HIS marker gene disruption cassette; Mutant II, mutant yeast strain without marker gene.
(TIF)

Figure S2   The IR spectra of fumaric acid. (a) sample; (b) the fumaric acid standard.
(TIF)

Figure S3   The ^{1}H and ^{13}C NMR spectrum of sample and the fumarate standard. (a) ^{1}H spectrum of the fumarate standard; (b) ^{13}C spectrum of the fumarate standard; (c) ^{1}H spectrum of sample; (d) ^{13}C spectrum of sample.
(RAR)

Table S1   The central metabolic flux of CEN.PK2-1CΔFUM1 was analyzed using iND750 and an FBA algorithm. The genome-scale analysis was divided into three types of intracellular flux profiles occur: increased, decreased and irregular. The "increased" represents that the flux increases when FA production successively increased, the "decreased" represents that the flux decreases when FA production successively increased, and the "irregular" represents that the flux is unchanged or ruleless when FA production successively increased.
(XLSX)

Author Contributions

Conceived and designed the experiments: GQX WZ XLC NX LML JC. Performed the experiments: GQX XLC. Analyzed the data: GQX WZ NX. Contributed reagents/materials/analysis tools: GQX XLC. Wrote the paper: GQX WZ.

References

1. Goldberg I, Rokem JS, Pines O (2006) Organic acids: old metabolites, new themes. Journal of Chemical Technology and Biotechnology 81: 1601–1611.
2. Cao N, Du J, Gong CS, Tsao GT (1996) Simultaneous production and recovery of fumaric acid from immobilized *Rhizopus oryzae* with a rotary biofilm contactor and an adsorption column. Appl Environ Microbiol 62: 2926–2931.
3. Kenealy W, Zaady E, du Preez JC, Stieglitz B, Goldberg I (1986) Biochemical aspects of fumaric acid accumulation by *Rhizopus arrhizus*. Appl Environ Microbiol 52: 128–133.
4. Abbott DA, Zelle RM, Pronk JT, van Maris AJ (2009) Metabolic engineering of Saccharomyces cerevisiae for production of carboxylic acids: current status and challenges. FEMS Yeast Res 9: 1123–1136.
5. Tokuhiro K, Ishida N, Nagamori E, Saitoh S, Onishi T, et al. (2009) Double mutation of the *PDC1* and *ADH1* genes improves lactate production in the yeast *Saccharomyces cerevisiae* expressing the bovine lactate dehydrogenase gene. Appl Microbiol Biotechnol 82: 883–890.
6. Zelle RM, de Hulster E, van Winden WA, de Waard P, Dijkema C, et al. (2008) Malic acid production by *Saccharomyces cerevisiae*: engineering of pyruvate carboxylation, oxaloacetate reduction, and malate export. Appl Environ Microbiol 74: 2766–2777.
7. Zelle RM, de Hulster E, Kloezen W, Pronk JT, van Maris AJ (2010) Key process conditions for production of C$_4$ dicarboxylic acids in bioreactor batch cultures of an engineered *Saccharomyces cerevisiae* strain. Appl Environ Microbiol 76: 744–750.
8. Raab AM, Gebhardt G, Bolotina N, Weuster-Botz D, Lang C (2010) Metabolic engineering of *Saccharomyces cerevisiae* for the biotechnological production of succinic acid. Metab Eng 12: 518–525.
9. Raab AM, Hlavacek V, Bolotina N, Lang C (2011) Shifting the fermentative/oxidative balance in *Saccharomyces cerevisiae* by transcriptional deregulation of Snf1 via overexpression of the upstream activating kinase Sak1p. Appl Environ Microbiol 77: 1981–1989.
10. Xu G, Liu L, Chen J (2012) Reconstruction of cytosolic fumaric acid biosynthetic pathways in *Saccharomyces cerevisiae*. Microbial Cell Factories 11: 24.
11. Kaclikova E, Lachowicz TM, Gbelska Y, Subik J (1992) Fumaric acid overproduction in yeast mutants deficient in fumarase. FEMS Microbiol Lett 91: 101–106.
12. Park JH, Lee KH, Kim TY, Lee SY (2007) Metabolic engineering of *Escherichia coli* for the production of L-valine based on transcriptome analysis and *in silico* gene knockout simulation. Proc Natl Acad Sci U S A 104: 7797–7802.
13. Lee KH, Park JH, Kim TY, Kim HU, Lee SY (2007) Systems metabolic engineering of *Escherichia coli* for L-threonine production. Mol Syst Biol 3: 149.
14. Bro C, Regenberg B, Forster J, Nielsen J (2006) In silico aided metabolic engineering of *Saccharomyces cerevisiae* for improved bioethanol production. Metab Eng 8: 102–111.

15. Brochado AR, Matos C, Moller BL, Hansen J, Mortensen UH, et al. (2010) Improved vanillin production in baker's yeast through in silico design. Microbial Cell Factories 9: 84.
16. Lee JW, Kim TY, Jang YS, Choi S, Lee SY (2011) Systems metabolic engineering for chemicals and materials. Trends Biotechnol 29: 370–378.
17. Duarte NC, Herrgard MJ, Palsson BO (2004) Reconstruction and validation of Saccharomyces cerevisiae iND750, a fully compartmentalized genome-scale metabolic model. Genome Res 14: 1298–1309.
18. Orth JD, Thiele I, Palsson BO (2010) What is flux balance analysis? Nat Biotechnol 28: 245–248.
19. Edwards JS, Palsson BO (2000) Robustness analysis of the Escherichia coli metabolic network. Biotechnol Prog 16: 927–939.
20. Nevoigt E (2008) Progress in metabolic engineering of Saccharomyces cerevisiae. Microbiol Mol Biol Rev 72: 379–412.
21. Palmieri L, Lasorsa FM, De Palma A, Palmieri F, Runswick MJ, et al. (1997) Identification of the yeast ACR1 gene product as a succinate-fumarate transporter essential for growth on ethanol or acetate. FEBS Lett 417: 114–118.
22. Bojunga N, Kotter P, Entian KD (1998) The succinate/fumarate transporter Acr1p of Saccharomyces cerevisiae is part of the gluconeogenic pathway and its expression is regulated by Cat8p. Mol Gen Genet 260: 453–461.
23. Redruello B, Valdes E, Luz Lopez M, Rodicio R (1999) Multiple regulatory elements control the expression of the yeast ACR1 gene. FEBS Lett 445: 246–250.
24. Kim TY, Sohn SB, Kim YB, Kim WJ, Lee SY (2011) Recent advances in reconstruction and applications of genome-scale metabolic models. Curr Opin Biotechnol.
25. Liu LM, Agren R, Bordel S, Nielsen J (2010) Use of genome-scale metabolic models for understanding microbial physiology. Febs Letters 584: 2556–2564.
26. Oberhardt MA, Palsson BO, Papin JA (2009) Applications of genome-scale metabolic reconstructions. Mol Syst Biol 5: 320.
27. Durot M, Bourguignon PY, Schachter V (2009) Genome-scale models of bacterial metabolism: reconstruction and applications. FEMS Microbiol Rev 33: 164–190.
28. Raman K, Chandra N (2009) Flux balance analysis of biological systems: applications and challenges. Brief Bioinform 10: 435–449.
29. Osterlund T, Nookaew I, Nielsen J (2011) Fifteen years of large scale metabolic modeling of yeast: Developments and impacts. Biotechnol Adv.
30. Arikawa Y, Kuroyanagi T, Shimosaka M, Muratsubaki H, Enomoto K, et al. (1999) Effect of gene disruptions of the TCA cycle on production of succinic acid in Saccharomyces cerevisiae. J Biosci Bioeng 87: 28–36.
31. Frick O, Wittmann C (2005) Characterization of the metabolic shift between oxidative and fermentative growth in Saccharomyces cerevisiae by comparative ^{13}C flux analysis. Microbial Cell Factories 4: 30.
32. Gueldener U, Heinisch J, Koehler GJ, Voss D, Hegemann JH (2002) A second set of loxP marker cassettes for Cre-mediated multiple gene knockouts in budding yeast. Nucleic Acids Res 30: e23.
33. Guldener U, Heck S, Fielder T, Beinhauer J, Hegemann JH (1996) A new efficient gene disruption cassette for repeated use in budding yeast. Nucleic Acids Res 24: 2519–2524.
34. Schellenberger J, Que R, Fleming RM, Thiele I, Orth JD, et al. (2011) Quantitative prediction of cellular metabolism with constraint-based models: the COBRA Toolbox v2.0. Nat Protoc 6: 1290–1307.